

ChemComm

Accepted Manuscript



This is an *Accepted Manuscript*, which has been through the Royal Society of Chemistry peer review process and has been accepted for publication.

Accepted Manuscripts are published online shortly after acceptance, before technical editing, formatting and proof reading. Using this free service, authors can make their results available to the community, in citable form, before we publish the edited article. We will replace this *Accepted Manuscript* with the edited and formatted *Advance Article* as soon as it is available.

You can find more information about *Accepted Manuscripts* in the [Information for Authors](#).

Please note that technical editing may introduce minor changes to the text and/or graphics, which may alter content. The journal's standard [Terms & Conditions](#) and the [Ethical guidelines](#) still apply. In no event shall the Royal Society of Chemistry be held responsible for any errors or omissions in this *Accepted Manuscript* or any consequences arising from the use of any information it contains.

ARTICLE

Recent applications of carbon nanomaterials in fluorescence biosensing and bioimaging

Cite this: DOI: 10.1039/x0xx00000x

Jia Wen,^a Yongqian Xu,^a Hongjuan Li,^a Aiping Lu^{b*} and Shiguo Sun^{a*}

Received 00th January 2012,

Accepted 00th January 2012

DOI: 10.1039/x0xx00000x

www.rsc.org/

Carbon based nanomaterials as important agents for biological applications have emerged in past few years due to their unique optical, electronic, mechanical, and chemical properties. And many of these applications are rely on successful surface modifications. This review article is comprised of two main parts. In the first part, we briefly review the properties and surface modifications of several classes of carbon nanomaterials mainly carbon nanotubes (CNTs), graphene and its derivatives, carbon dots (CDs) and graphene quantum dots (GQDs) as well as some other forms of carbon-based nanomaterials such as fullerene, carbon nanohorns (CNHs) and carbon nanooxions (CNOs); in the second part, we focus on the biological applications of these carbon nanomaterials, in particular, the applications for fluorescence biosensing as well as bioimaging.

Introduction

In recent years, numerous classes of carbon nanomaterials such as carbon nanotubes (CNTs), graphene and its derivatives, carbon dots (CDs), graphene quantum dots (GQDs), fullerene, carbon nanohorns (CNHs) and carbon nanooxions (CNOs) have been explored for potential applications in the field of biology, owing to their unique physical and chemical properties. Among them, CNTs, graphene and its derivatives, CDs, GQDs as well as their nanocomposites are subjects of fundamental research.

CNTs consist of carbon atoms arranged in one (single-walled carbon nanotubes: SWCNTs)¹ or more (multiwalled carbon nanotubes: MWCNTs)² graphene sheets and rolled up to form a cylinder.³ CNTs are nanostructures with excellent properties, including high surface area, rigid structure, and good electrical conductivity,⁴ making them appealing for biological agents. Owing that, biological applications of carbon nanotubes, such as biosensing, bioimaging, drug delivery, therapy are emerging

in recent years.⁵⁻⁸ Since the discovery of graphene by Geim *et al.*⁹ in 2004, graphene and its derivatives such as graphene oxide (GO), reduced graphene oxide (RGO) and GO-nanocomposites have attracted significant interest owing to their unique optical, structural, chemical and electronic properties.¹⁰⁻¹² Especially in the area of biology, graphene-based materials have attracted tremendous interest in recent years.¹³⁻¹⁹ Owing to their specific and large surface area, graphene and its derivatives can interact with various biomolecules such as DNA, proteins and the like for applications in biosensing, bioimaging, drug delivery and so on.²⁰⁻²³ CDs are a new form of zero-dimensional carbonaceous nanomaterials,²⁴⁻²⁷ which are first obtained during purification of SWCNTs via preparative electrophoresis in 2004.²⁸ They are quasi-spherical carbon nanoparticles with a diameter of less than 10 nm. Compared to conventional semiconductor quantum dots (QDs), CDs are superior in terms of low cytotoxicity and excellent biocompatibility.²⁹⁻³¹ Therefore, CDs have been widely used in biosensing and bioimaging.³²⁻³⁶ As a kind of CDs, GQDs, not only have the properties of CDs but also have the excellent performance of graphene. In recent years, GQDs are also enormously used in biosensing, bioimaging, drug delivery and so on.³⁷⁻⁴⁴ Some other classes carbon nanomaterials such as fullerenes which are the zero-

^a College of Science, Northwest A&F University, Yangling, Shaanxi, 712100, China, E-mail: sunsg@nwsuaf.edu.cn.

^b School of Chinese Medicine, Hong Kong Baptist University, Kowloon Tong, Hong Kong, 999077, China, E-mail: aipinglu@hkbu.edu.hk.

dimensional form of graphitic carbon and can be visualized as an irregular sheet of graphene being curled up into a sphere by incorporating pentagons in its structure;⁴⁵ CNHs which appear as conical, single-walled carbon nanostructures related to CNTs;⁴⁶ CNOs which consist of several individual spherical graphitic layers of carbon usually with a fullerene C₆₀ or its larger analogues in the centre,⁴⁷ also have exceptional physical and chemical properties as well as can be implemented for fluorescence biosensing and bioimaging.

Recent research trends show focusing effects on the biological applications of these carbon nanomaterials (Fig. 1). In this review article, we will focus on the properties and surface modifications, the latest biological applications especially biosensing and bioimaging, as well as future prospects of these main carbon nanomaterials.

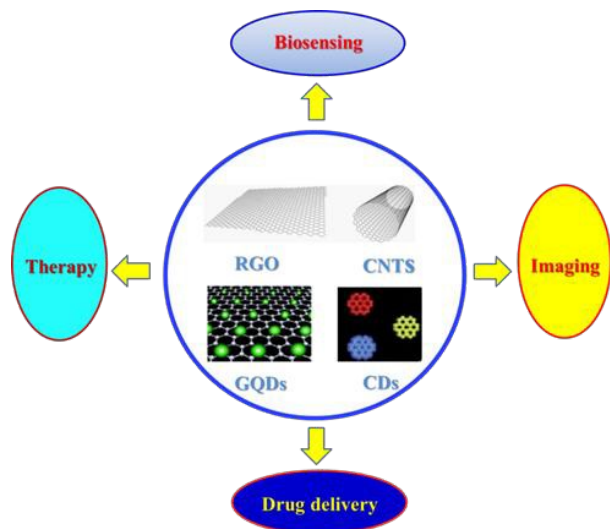


Fig. 1 Examples of carbon nanomaterials for biological applications.

Modifications of carbon nanomaterials

Owing to their exceptional physical and chemical properties, CNTs,⁴⁸ graphene and its derivatives, CDs,^{37, 49-52} GQDs,^{37-44, 53-54} fullerene, CNHs and CNOs have attracted great interest in many different fields including biology in recent years. What's more, most of biological applications of carbon nanomaterials are rely on the modifications. In order to improve the properties of carbon nanomaterials, the modification of carbon nanomaterials is emerging. Many applications of carbon nanomaterials depend on the successful modifications which are mainly classified into two categories: covalent modifications and noncovalent modifications. Here we briefly discuss the covalent and noncovalent approaches to modify carbon nanomaterials mainly CNTs, graphene and its derivatives, CDs, GQDs. For detail, the readers may refer to several previous articles on this topic.⁵³⁻⁵⁷

Covalent modifications.

For CNTs, the covalent modifications are mostly applied via chemical reactions like oxidations, halogenations,

cycloadditions or electrochemical reactions.⁵⁸ These reactions can change the shape and even structures of CNTs, or change the length of CNTs, or create some chemical groups on the edge of CNTs.⁵⁹ The covalent modifications mostly enhance the biocompatibility and hydrophilic of CNTs and are hence widely used in biology and medical research. For graphene and its derivatives, some chemical groups, commonly, carboxylic (–COOH) and hydroxyl (–OH) groups, can be covalently added on their surface using strong acids and/or oxidants. The chemical groups created on the graphene and its derivatives' surface are used as chemical handles to graft functional molecules like proteins, carbohydrates, polymers through covalent bonding, hence increasing the biocompatibility, sensitivity and specificity of graphene and its derivatives. Yan *et al.*⁶⁰ modified graphene with perfluorophenylazide (PFPA) through photochemical or thermal activation, successfully synthesizing graphene with well-defined functionalities whose solubility in organic solvents or water depended on the properties of the functional group on PFPA. For CDs, owing to their easy functionalization, there are many ways to modify CDs through the surface chemistry or interactions. The modifications of CDs not only tune or enhance the luminescence but also make them superior for biological applications. For example, Liu and co-workers⁶¹ fabricated a kind of amino-functionalized CDs with low cytotoxicity and excellent biocompatibility through hydrothermal carbonization of chitosan, which were applied for bioimaging in cells. Like CDs, GQDs also can be modified through many methods. Modification of the GQDs can not only improve their properties further but also provide a way to modulate their properties.⁶²⁻⁶⁴ As an example, Zhang *et al.*⁶⁵ reported a new strategy to prepare GQDs in mass scale by modified GQDs with carboxylic groups through Fenton reagent (Fe²⁺/Fe³⁺/H₂O₂) under an UV irradiation.

Noncovalent modifications.

However, covalent modifications will affect or even destroy the microstructure and properties of carbon nanomaterials to some extent. To avoid this shortage, noncovalent modification is emerging as an important way to modify carbon nanomaterials. Because of their benzene ring structures, CNTs can noncovalently interact with aromatic polymers or biomolecules through π – π stacking, electrostatic interactions, van der Waal's forces, hydrogen bonding and so on. These advantages provide approaches to control biological behavior, such as the toxicity and biocompatibility of CNTs. For example, Sansom and co-workers have modified a designed amphiphilic peptide helix on CNTs which successfully enhancing the selective solubilisation and manipulation of CNTs.⁶⁶ Wallace *et al.*⁵³ used an aligned CNT array membrane electrode as a nanostructured supporting platform for polypyrrole (PPy) films, significantly improving the controlled release of neurotrophin. Graphene and its derivatives which are highly negatively charged, are able to electrostatically adsorb oppositely charged molecules. In addition, π – π stacking, hydrophobic or van der Waals interaction may assist the physical adsorption. Through this process, some biomolecules like single-stranded

DNA (ssDNA) can be anchored on graphene or its derivatives.⁶⁷⁻⁷⁶ For example, Ju *et al.*⁷² have successfully used polyethylenimine-modified graphene as a vector for in situ detection of gene and gene therapy. There are also many ways to modify CDs and GQDs through noncovalent interactions, such as π - π interactions,⁷⁷ hydrophobic interactions, van der Waals interaction and so on.

Carbon nanomaterials for fluorescence biosensing

Owing to the sensitivity of the biological and chemical properties of carbon nanomaterials to the surrounding environment, it provides an exceptional advantage for biosensors. In recent years, carbon nanomaterials have been used to sense a variety of analytes including biomolecules, gases and solvents. A majority of them are by means of fluorescence. In this section, we will review some of the achievements of the successful fluorescence biosensing based on carbon nanomaterials mainly CNTs, graphene and its derivatives, CDs, GQDs in recent five years.

CNTs for fluorescence biosensing

In recent years, biosensing based on CNTs have called enormous attention of scientists because of their advantages, such as a broad absorption spectrum, low background, high signal-to-noise ratio, label-free detection, real-time monitoring, high sensitivity, and simplicity of apparatus. CNTs also have an ultrahigh surface area for loading multiple molecules achieving multiplexed sensing. Meanwhile, CNTs attached by nucleic acids or proteins⁷⁸ can protect these biomolecules from enzymatic digestion or degradation in the biological environment. Given these properties in relation to the design of fluorescence biosensing system, CNTs have become a promising candidate for fluorescence biosensing. Many groups including us have devoted to exploring CNTs-based biosensing systems. As follows, we demonstrate some specific examples. Liang *et al.*⁷⁹ have developed an amplified chemiluminescence turn-on sensing platform for ultrasensitive DNA detection which depended on SWCNTs. The sensing platform was based on the modulation in chemiluminescence resonance energy transfer (CRET) efficiency between the SWCNTs acceptor and the chemiluminescent donor. The chemiluminescence of the sensor was switched on by the exonuclease-recycled DNA cleavage and turned off by CRET on the SWCNTs surface, thus, resulting in the amplification of the read-out signal, obtaining three orders of magnitude detection sensitivity over traditional biosensors and higher specificity for the target molecules (Fig. 2).

In our previous work,⁸⁰ the SWCNTs was used to quench the fluorescence of acridine orange (AO), due to the formation of a hybrid complex between AO and SWCNTs. Approximately 18-times fluorescence enhancement can be observed after the addition of certain amount of DNA into the above mentioned solution. The fluorescence increase was linearly proportional to the amount of DNA added in the concentration range of 0-50.75 μ M, and the limit of detection (LOD) of DNA was down

to 8.56×10^{-8} M. Huang *et al.*⁸¹ have successfully constructed a novel and efficient method for the label-free and turn-on fluorescent detection of the respiratory syncytial virus gene sequence with a LOD of 24 nM based on the fluorescence resonance energy transfer (FRET) between MWCNTs and DNA-AgNCs. The notable fluorescence enhancement of the DNA-AgNCs resulted from the specific binding of DNA-AgNCs with target DNA and the quench of the fluorescence of the DNA-AgNCs with an extraordinarily high quenching efficiency (85.8%) resulted from MWCNTs.

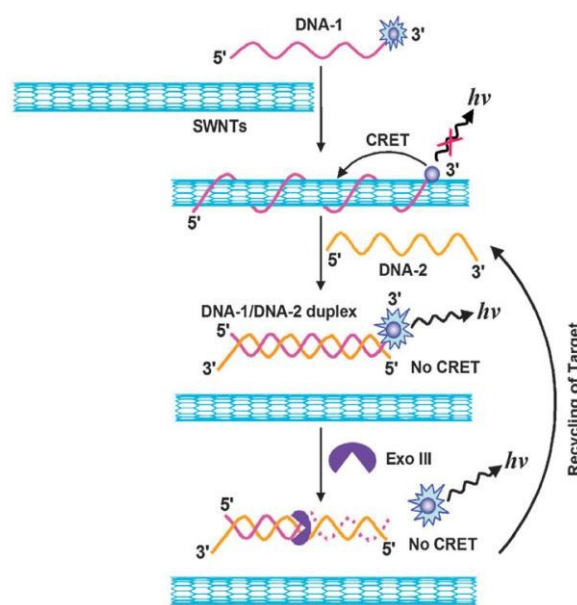


Fig. 2 Schematic illustration of the sensing principle with the proposed amplified SWCNT-mediated CRET platform for DNA detection. Copyright 2012 Royal Society of Chemistry.⁷⁹

CNTs are widely used for the highly specific and rapid detection of target proteins owing to their large binding surface area. Recently, Kwon *et al.*⁸² have fabricated horizontally aligned carbon nanotubes (ACNTs), which were functionalized with specific aptamers with ability to specifically bind to biomolecules such as thrombin. The detection system was based on scanning probe microscopy (SPM) imaging for ACNTs that specifically reacted with target biomolecules at an ultra-low concentration with a high detection sensitivity to 1 pM.

Moreover, many of biosensing systems are based on the change in the near-infrared (NIR) emission spectra of the CNTs. Their fluorescence in the NIR region (between 820 and 1600 nm), where absorption of biological tissues is usually negligible, inherent photostability and tissue transparency are exceptional characteristics for the design of in vitro and in vivo sensors. As an example, Yudasaka *et al.*⁸³ demonstrated an immunoassay by using a NIR CNT labels conjugated to immunoglobulin G (IgG) antibodies. The NIR emission of the conjugated CNTs at 1000–1200 nm confirmed that most of the CNT-conjugated IgG was successfully immunoprecipitated with protein G-attached magnetic beads and eluted from them. For

result, the photoluminescence intensity of the CNT labels was strong enough to detect antigens at 600 pM by above-mentioned procedures.

Moreover, some of the applications based on the development of glucose sensors. For example, Dasgupta and co-workers⁸⁴ have exploited a lipid functionalized SWCNT-based self-assembly super-micellar structure to trap glucose oxidase in a molecular cargo for glucose sensing. The remarkable feature of such a molecular trap is that all components of this unique structure are reusable and rechargeable. What's more, the glucose sensing was achieved without any hybrid fabrication.

Similarly, CNTs are widely used to detect nitric oxide (NO) due to their high surface area. The ability to detect NO quantitatively may assist the study of NO carcinogenesis and chemical signaling, as well as medical diagnostics for inflammation. Strano *et al.*⁸⁵ reported the selective detection of single NO molecules based on a specific DNA sequence of d(AT)₁₅ oligonucleotides, adsorbed to an array of NIR fluorescent semiconducting SWCNTs (AT₁₅-SWCNT). When the sensor was exposed to NO, a stepwise fluorescence decrease was observed and these quenching traces were described by using a birth and-death Markov model, whose maximum likelihood estimator reported the adsorption and desorption rates of NO. The adsorption rate showed a linear dependence upon NO concentration.

Graphene for fluorescence biosensing

On the basis of their fluorescence and quenching abilities, graphene and its derivatives can serve as either an energy donor or acceptor in a FRET sensor. They have been extensively investigated for the sensing of DNA, protein or other biomolecules, detection of single-base mismatches, analysis of the melting of DNA duplexes and so on.⁸⁶⁻⁸⁹ For the detection of DNA, Lin *et al.*⁹⁰ reported a GO based fluorescence quenching-recovery sensor to detect ssDNA with a LOD of nM range. Because of ssDNA retained on the GO surface was indigestible by DNAase, their sensors can perform even in the presence of DNAase. Two similar DNA sensors, with ability to distinguish single-base-mismatch, have also been exploited.^{91, 92} In our recent research, a hybrid graphene/ZnAl-LDH nanocomposite has been fabricated via a one-step process and used as a facile shelf of the Ru(phen)₃Cl₂ (tris(1,10-phenanthroline)ruthenium(II) dichloride) sensor to selective DNA. Moreover, both of the shelf and the sensor can be easily collected and used for the next sample if no DNA existed in the solution.⁹³ Some researchers have combined graphene and its derivatives with noble metal nanoparticles to induce a double-quenching effect that resulted in an increase in the achievable signal-to-noise ratio hence obtaining the amplification of the achievable sensitivity. For example, Ren *et al.*⁹⁴ reported a DNA-silver nanocluster-GO nanohybrid material for the detection of multiple nucleic acid targets with low LOD and high sensitivity and selectivity, which was attributed to the high achievable signal-to-noise ratio resulting from the high quenching efficiency of GO.

Graphene and its derivatives are also widely used for fluorescence biosensing of proteins. For example, In our previous work,⁹⁵ chemically converted graphene (CCG) was utilized to effectively quench the fluorescence emission of Cy3 dye **1** (the intensity is down to 1/38 of **1** alone) in aqueous solution (Fig. 3). After the addition of a certain amount of bovine serum albumin (BSA), about 60 times fluorescence enhancement was observed for the hybrid CCG-**1**. This was employed to discriminate BSA: the fluorescence intensity was found to be proportional to the BSA added in the concentration range from 0 to 8×10⁻⁶ M, and the LOD of BSA was down to 5×10⁻⁸ M.

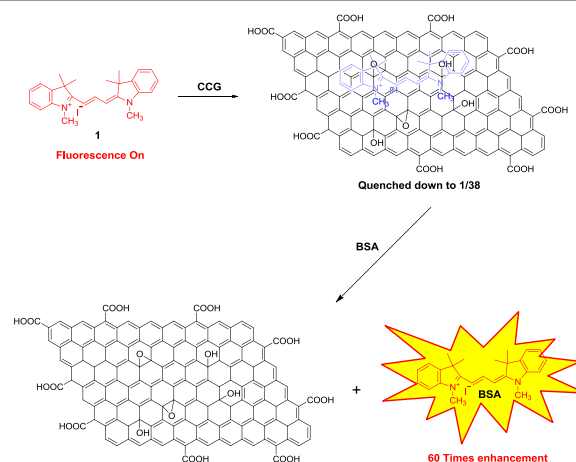


Fig. 3 Schematic illustration of the fluorescence detection of BSA using the hybrid of **1** and CCG. Copyright 2013 Royal Society of Chemistry.⁹⁵

Huang's group designed a simple, selective and sensitive fluorescent GO-based molecular aptamer beacon (MAB) for PrP^C detection via using GO as a quenching reagent.⁹⁶ As a result, the TAMRA-labelled MAB moved away from the surface of GO, and the fluorescence of MAB was recovered. Owing to the high energy transfer efficiency between the GO and the fluorophore, the background signal was significantly reduced. Also for the detection of PrP^C, the authors then developed a new FRET strategy via using QDs as the energy donor and GO as the energy acceptor through the specific recognition between the two binding aptamers and PrP^C with high sensitivity and good selectivity.⁹⁷ The detection signals were greatly improved by the high FRET efficiency between QDs and GO.

Graphene and its derivatives have been enormously used in other biosensing applications like enzymatic reaction monitoring and biomacromolecules detection. Nie *et al.*⁹⁸ proposed a novel and versatile biosensing platform for the detection of protein kinase activity based on GO-peptide nanocomplex and phosphorylation-induced suppression of carboxypeptidase Y (CPY) cleavage. Kinase catalyzed phosphorylation protected the fluorophore-labeled peptide probe against CPY digestion and induced the formation of a GO-peptide nanocomplex resulting in fluorescence quenching, while the nonphosphopeptide was degraded by CPY to release free fluorophore thus restoring fluorescence. This GO-based

nanosensor has been successfully applied to sensitively detect two model kinases, casein kinase (CKII) and cAMP-dependent protein kinase (PKA) with low LOD of $0.0833 \text{ mU } \mu\text{L}^{-1}$ and $0.134 \text{ mU } \mu\text{L}^{-1}$, respectively. Li *et al.*⁹⁹ reported a versatile biosensing platform capable of achieving ultrasensitive detection of both small-molecule and macromolecular targets. The system consisted of three parts: a nanomaterial (graphene), a biomaterial (DNA aptamers), and an isothermal signal amplification technique (RCA). Graphene was chosen for its ability to adsorb ssDNA molecules nonspecifically. The key to the design was grafting a short primer to an aptamer sequence, which resulted in a small DNA probe that allowed for both effective probe adsorption onto the graphene surface to mask the primer domain in the absence of the target and efficient probe release in the presence of the target to make the primer available for template binding and RCA. The detection was highly sensitive and feasible for protein target, DNA sequence and small-molecule analyte.

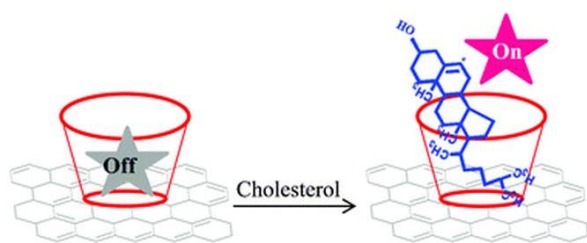


Fig. 4 Schematic illustration of the fluorescence detection of cholesterol by using of the fluorescence of β -CD incorporated R6G. Copyright 2012 Royal Society of Chemistry.¹⁰¹

Glucose detection is clinically significant for diagnosis and management of diabetes. Its detection can be realized by using graphene and its derivatives as the mediator. Wang *et al.*¹⁰⁰ demonstrated an efficient biosensing system for glucose detection based on enzyme like activity of graphene oxide integrated with chitosan. The chitosan-functionalized graphene oxide (CS-GO) hybrid was demonstrated to be a good enzyme mimetic for oxidation of a typical substrate (TMB) under visible light ($\lambda \geq 400 \text{ nm}$) stimulation and was independent of destructive hydrogen peroxide. Avijit Mondal and Nikhil R. Jana developed a fluorescence based cholesterol detection method using competitive host-guest interaction between graphene bound β -cyclodextrin (β -CD) with rhodamine 6G (R6G) and cholesterol (Fig. 4). Fluorescence of β -CD incorporated R6G was quenched by graphene but was restored by cholesterol as it replaced R6G from the β -CD host.¹⁰¹

CDs for fluorescence biosensing

Based on their excellent properties, CDs have been applied for biosensing as fluorescent labels for DNA, aptamers, proteins, glucose, phosphate, metal ions and so on.¹⁰²⁻¹¹⁶ As for the detection of nucleic acids, Sun *et al.*⁷⁷ demonstrated an effective fluorescent sensing platform for nucleic acid detection using CDs. The dye-labeled ssDNA probe was

adsorbed onto the surface of the CDs via π - π interaction, quenching the dye. A double-stranded DNA (dsDNA) hybrid formed, recovering dye fluorescence. Kim and co-workers¹¹⁷ successfully prepared a CDs-based miR124a imaging sensor with no evidence of cellular toxicity and a high level of self-promoted uptake into cells. The CDs-based miR124a molecular beacon (CMB) was easily internalized into P19 cells and successfully visualized a gradual increase in miR124a expression during neuronal differentiation by providing signal-on imaging activity. The CDs were purified from candle soot (cCDs) by thermal oxidation. The dsDNA oligonucleotide containing a miR124a binding site and black hole quencher 1 (miR124a sensing oligo) was further conjugated with the cCDs to form the miR124a CMB. P19 cells were incubated with the miR124a CMB to sense miR124a expression during neurogenesis.

Another kind of application is based on the exploitation of aptamers. The aptamers are usually based on a conformational change induced by the target and could result in a detectable change in response. Qu *et al.*¹¹⁸ developed an aptamer-CDs-based sandwich system for sensitive and selective detection of thrombin with a LOD of 1 nM (Fig. 5). The presence of thrombin can induce the aptamer-modified fluorescent CDs to form a sandwich structure with aptamer-functionalized silica nanoparticles through specific protein/ aptamer interaction.

The concept of fluorescence intensity changes is also applied to the detection of proteins. Das *et al.*¹¹⁹ developed a fluorimetric histone sensing technique with a LOD of 0.2 ng mL^{-1} via using quaternized carbon dot (QCD)-DNA nanohybrid for the first time. The QCD-ds-DNA hybrid was prepared through electrostatic attraction. The emission of the QCD was quenched in presence of ds-DNA but recovered through the addition of histone to this QCD-ds-DNA hybrid due to the strong binding affinity between histone and ds-DNA.

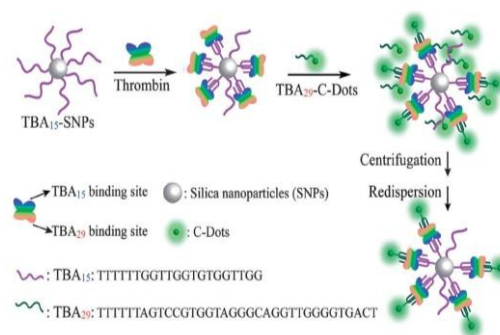


Fig. 5 Schematic illustration of the sandwich-based thrombin detection principle using the CDs. Copyright 2012 Royal Society of Chemistry.¹¹⁸

In addition to biomolecules, CDs have also shown promise as fluorescent probes in the detection of small bioanalytes like anti-bacterial drugs, dopamine (DA), ascorbic acid (AA), glucose and so on. For example, Niu's group¹¹⁴ synthesized a new type of eco-friendly molecularly imprinted polymer (MIP) through an efficient one-pot room-temperature sol-gel polymerization and applied it as a molecular recognition

element to construct DA fluorescence optosensor. The new MIP-based DA sensing protocol was successfully applied to detect DA concentration in aqueous solution with a LOD of 1.7 nM as well as in human urine samples without the interference of other molecules and ions. Sun *et al.*¹¹³ demonstrated an on-off fluorescent CD probe of simplicity, convenience, rapid response, high selectivity, and sensitivity, for detecting Cr(VI) based on the inner filter effect (IFE) because the absorption bands of Cr(IV) fully covered the emission and excitation bands of CDs. They successfully employed AA as an example molecule to demonstrate this off-on type fluorescent probe. S. Kiran and R. D. K. Misra demonstrated a new class of "inert" non-enzymatic and boronic acid functionalized CDs-based sensors facilitating intracellular detection of glucose.¹²⁰ The study suggested that the mechanism of detection of glucose involved selective assembly and fluorescence quenching of the CDs with excellent dynamic response to varying concentration of glucose within the biological range (1–100 mM). The strong dynamic response was related to high selectivity to biomolecules and inertness of CDs.

GQDs for fluorescence biosensing

GQDs not only have the good properties of CDs but also possess some of the excellent properties of graphene, such as good electron mobility and chemical stability. They are also widely used for biosensing.^{40, 121-126} The fluorescence of GQDs can be effectively quenched by selectively interacting with specific cations, anions, or chemical groups.¹²⁷⁻¹³¹ This feature allows GQDs to be used as sensors to detect nucleic acids. For example, Feng *et al.*¹³² established a novel and effective fluorescent sensing platform for the detection of DNA based on FRET, by regulating the interaction between GO and GQDs for the first time. It can be used as a universal strategy for DNA detection as well as can distinguish complementary and mismatched nucleic acid sequences with high sensitivity and good reproducibility.

What's more, GQDs also can be used as sensors to detect various biomolecules like proteins. Chen *et al.*¹³³ synthesized a kind of highly blue-luminescent nitrogen-doped graphene quantum dots (N-GQDs) with quantum yield (QY) as high as 32.4% via a facile one-step hydrothermal treatment of citric acid and dicyandiamide. The as-prepared N-GQDs can be used as efficient fluorescent probes for the detection of glutathione (GSH) with a LOD of 87 nM. Yu *et al.*¹³⁴ developed a facile method for the highly sensitive and selective sensing of biothiols based on GQDs with strong blue fluorescence in an aqueous buffer solution. It was observed that mercury(II) ions could efficiently bind and quench the fluorescence of the GQDs. When a biothiol compound (glutathione, cysteine, or homocysteine) was added to the assay mixture of GQDs and mercury(II), it bound to mercury(II) ions. Hg^{2+} -GQD complex dissociated, and fluorescence restored. The emission intensity changes of the GQDs could be directly related to the amount of biothiol added to the assay solution. The LOD for GSH, Cys and Hcy were 5 nM, 2.5 nM and 5 nM, respectively.

In addition to biomacromolecules, GQDs have also shown promise as fluorescent probes in the detection of small bioanalytes like glucose. For example, Yang *et al.*¹³⁵ proposed a DNA-mediated silver nanoparticle and graphene quantum dot hybrid nanocomposite (AgNP-DNA@GQDs) for sensitive fluorescent detection of H_2O_2 and glucose (Fig. 6). The sensing mechanism was based on the etching effect of H_2O_2 to AgNPs and the cleavage of DNA by as-generated hydroxyl radicals ($\bullet\text{OH}$). The formation of AgNP-DNA@GQDs nanocomposite can result in fluorescence quenching of GQDs by AgNPs through the resonance energy transfer. Upon H_2O_2 addition, the energy transfer between AgNPs and GQDs mediated by DNA was weakened and obvious fluorescence recovery of GQDs could be observed. For the oxidation of glucose and formation of H_2O_2 , this nanocomposite can be further extended to the glucose sensing in human urine combining with glucose oxidase (GOx). The glucose concentrations in human urine were detected with satisfactory recoveries of 94.6–98.8% which held potential for ultrasensitive quantitative analysis of glucose.

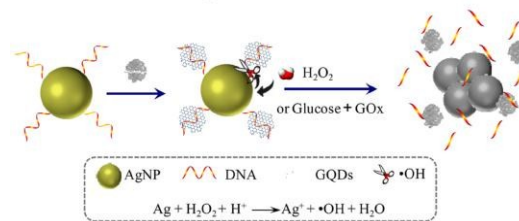


Fig. 6 Schematic description of H_2O_2 and glucose detection based on AgNP-DNA@GQDs. Copyright 2014 American Chemical Society.¹³⁵

Carbon nanomaterials for bioimaging

As materials with high aqueous solubility, good biocompatibility, low cytotoxicity as well as superior resistance to photobleaching, carbon nanomaterials show great potential for fluorescent bioimaging and multimodal bioimaging of cells and tissues. In this section, we will discuss the use of carbon nanomaterials for bioimaging in recent five years.

CNTs for bioimaging

CNTs not only can be applied for fluorescence biosensing, but also can be used for fluorescence bioimaging further. In recent years, CNTs have been widely studied as in vitro and in vivo imaging agents.^{136, 137} For example, Kaeriyama *et al.*¹³⁸ demonstrated a simple approach for cell specific imaging and diagnosis by combining the folic acid (FA) treated carboxyl functional SWCNTs with a copolymer poly(para-phenylene) (PPP) containing polystyrene (PSt) and poly(ϵ -caprolactone) (PCL) side chains (PPP-g-PSt-PCL) via π - π stacking reactions. The conjugates which bound to FA can specifically target HeLa cells and possess great potential for targeting and imaging studies. Hassan *et al.*¹³⁹ introduced a novel method for in vivo imaging of the biodistribution of SWCNTs labeled recombinant thermo-stable *Luciola cruciate* luciferase (LcL). They demonstrated for the first time that LcL chemically bound to

SWCNTs was a powerful tool for CNTs in vivo imaging applications. Moreover, they also showed that the loading of CNTs with drugs did not inhibit the chemiluminescence of LCL. Banerjee *et al.*¹⁴⁰ have synthesized a highly versatile multifunctional nanosystem by covalently assembling Fe₃O₄ nanoparticles, polyethylene glycol (PEG), and fluorescein isothiocyanate (FITC) dye on CNTs for fluorescence bioimaging both in vitro and in vivo. In vitro time kinetic experiments using confocal microscopy demonstrated a higher uptake of the Fe₃O₄-PEG-FITC-CNT nanosystem localized at the perinuclear region of MCF7 cells compared to the free FITC. In addition, the CNT nanosystem demonstrated no evidence of toxicity on cell growth. In vitro, surface conjugation of multicomponents enhanced cellular uptake for FITC and site specific targeting ability with non-toxicity.

What's more, Raman imaging is one of the most promising and powerful bioimaging form of CNTs.⁴⁸ NIR excitation for Raman imaging can make one to minimize autofluorescence of biological specimen and/or photobleaching of CNTs. Recently, a versatile immunoassay using biotinylated SWCNTs as a Raman label was reported by Musselman and co-workers.¹⁴¹ They used avidin-biotin to link targeting ligands to the label, and confocal Raman microscopy to image whole cells. Shen *et al.*¹⁴² reported a flexible nanoplatfrom based on electrostatic assembly of conjugated polyelectrolytes (CPEs) and carboxylated multi-walled carbon nanotubes (cMWNTs). The obtained nanocomposites inherited intrinsic optical properties of CPEs and characteristic Raman vibration modes of MWNTs, providing a fluorescence-Raman dual-imaging method for intracellular tracking and locating of MWCNTs both in vitro and in vivo applications.

CNTs are also widely used for magnetic resonance imaging (MRI). Wu and co-workers¹⁴³ developed a simple and novel layer-by-layer (LBL) assembly in combination with covalent connection strategy for the synthesis of multifunctional CNTs-based magnetic-fluorescent nanohybrids as multimodal cellular imaging agents for detecting human embryonic kidney (HEK) 293T cells via MRI and confocal fluorescence imaging with higher intracellular labeling efficiency due to the ability of CNTs for penetrating into cells.

CNTs have great potential for effective drug delivery. The large surface area, availability of multiple functional groups and the hydrophobic nature are advantages of CNTs for loading and delivering drugs, proteins, DNA, and siRNA including fluorophores efficiently.¹⁴⁴⁻¹⁴⁹ Owing that, many biological applications have been made for CNTs combined drug delivery and bioimaging. What's more, through modification, CNTs offer more advantages such as bigger drug-loading capacity, high cell internalization, selective targeting and imaging. There are many biological applications of CNTs for bioimaging combined with drug delivery. For example, Yong *et al.*¹⁵⁰ have reported PEG modified SWCNTs as a nanocarrier for siRNA delivery into pancreatic cancer cells. The positively charged SWCNTs were complexed with siRNAs for targeting the mutant K-Ras gene in PANC-1 cells by electrostatic interaction, thereby promoting gene therapy. A

high siRNA transfection efficiency mediated by the nanoplex formulation was observed through fluorescent imaging and quantitative flow cytometric analysis.

Also, CNTs offer excellent photo-to-acoustic conversion efficiency and photothermal-acoustic response, making them one of the most promising contrast agents in photoacoustic imaging of tumors. Recently, Cui *et al.*¹⁵¹ reported for the first time that RGD-conjugated silica-coated gold nanorods on the surface of MWCNTs were successfully used for targeted photoacoustic imaging of gastric cancer cells in vivo. The RGD-conjugated silica-coated gold nanorods/MWCNT probes with good water solubility and low cellular toxicity could target gastric cancer cells in vivo as well as obtain strong photoacoustic imaging in the nude model. Gambhir's group¹⁵² presented a family of novel photoacoustic contrast agents based on the binding of small optical dyes to SWCNTs (SWCNT-dye). They found that SWCNTs coated with either QSY₂₁ (SWCNT-QSY) or indocyanine green (SWCNT-ICG) exhibited over 100-times higher photoacoustic contrast in living animals with high sensitivity compared to plain SWCNTs. Then they conjugated the SWCNT-dye with cyclic Arg-Gly-Asp peptides to molecularly target the $\alpha_v\beta_3$ integrin, which was associated with tumor angiogenesis. Intravenous administration of these tumor-targeted imaging agents to tumor-bearing mice showed significantly higher photoacoustic signal in the tumor than in mice injected with the untargeted contrast agent. They also were able to spectrally separate the photoacoustic signals of SWCNT-QSY and SWCNT-ICG in living animals injected subcutaneously with both particles in the same location, opening the possibility for multiplexing in vivo studies.

Graphene for bioimaging

Owing to their intrinsic physical especially optical properties, graphene and its derivatives not only can be used as biosensors but also can be applied in bioimaging meanwhile. The excellent optical properties of graphene and its derivatives such as the visible and NIR photoluminescence, characteristic Raman bands, and photo-acoustic and photothermal responses¹⁵³ make them attractive for bioimaging, especially in live cells. Thus, a lot of efforts have been devoted to exploiting graphene and its derivatives as fluorescent probes for intracellular imaging in vitro and in vivo.^{42, 154-158} For example, in 2013, our group developed a method to detect and image DNA in vivo via GO-Ru hybrid.¹⁵⁹ GO was employed to effectively quench the fluorescence of Ru(phen)₃Cl₂ via π - π interaction and electrostatic interaction, as well as load and delivery Ru(phen)₃Cl₂ into living cells nuclei to detect and image DNA, while Ru(phen)₃Cl₂ alone cannot enter into cells. Similarly, we successfully employed GO to delivery propidium iodide for live cell imaging.¹⁶⁰ Chen and co-workers¹⁶¹ reported that semiconductor QDs with strong fluorescence could be tagged to water-soluble polypeptide modified RGO, obtaining QD-RGO nanocomposites with largely retained QD fluorescence because of a suitable nanosized spacer separating QDs and RGO, which was useful in cell imaging.

Analogously, Wang *et al.*¹⁶² reported that gold nanoclusters with NIR photoluminescence were anchored on RGO and used for cell imaging. Xue *et al.*¹⁶³ reported a portable method to prepare fluorescent nanocomposites incorporating water-soluble GO sheets and Zn doped AgInS₂ nanoparticles. The PEGylated AIZS-GO nanocomposites could be easily up-taken by NIH/3T3 cells (mouse embryonic fibroblast cell line) while no distinct cytotoxicity was observed. Moreover, this as-prepared AIZS-GO-PEG nanocomposites could be used for in vitro cellular imaging of NIH/3T3 cells. Further, graphene and its derivatives also can be used for MRI. For instance, by growing iron oxide nanoparticles (IONP) on the surface of GO, a large number of groups have successfully fabricated superparamagnetic GO-IONP nanocomposites which could be employed as anticancer drug carriers as well as contrast agents in MRI.^{158, 164}

The large surface area, two dimensional π -stacked structure and CNT-like surface chemistry allow graphene and its derivatives to chemically conjugate or physically adsorb a large amount of cargos such as anticancer drugs.¹⁶⁵⁻¹⁷⁴ Contacting the excellent optical properties of graphene and its derivatives, many applications have been made for bioimaging meanwhile delivering drug. For example, Zhao and co-workers¹⁷⁵ have successfully fabricated graphene oxide wrapped gold nanoparticles (Au@NGO) by one-step. Surface enhanced Raman scattering from the Au@NGO nanoparticles was utilized for intracellular Raman imaging in HeLa cells. The Au@NGO nanoparticles could also serve as a carrier for anticancer drug delivery with sustained intracellular drug release in cancer treatment. In 2011, a real time method for monitoring the drug load and release on GO in a cuvette is reported using rhodamine B (RB) as a drug model by Zhang *et al.*¹⁷⁶ RB can be loaded on GO with a capacity of 0.5 mg mg⁻¹. The release of RB was pH sensitive, showing that higher pH values led to a weaker hydrophobic force and hydrogen bonding interactions, and thus higher rate of releasing. Some biomolecules can also be transported by conjugating with graphene and its derivatives and this process is visual based on fluorescence bioimaging. Huang *et al.*¹⁷⁷ developed a novel, multifunctional aptamer-QD-GO nanocomposite via a facile decoration of aptamer-labelled CdSe@ZnS QDs on GO nanosheets (Fig. 7). The formation of such nanocomposites was based on the π - π stacking between the DNA bases on the QD surfaces and the GO. The QDs decorated on the surfaces of GO could serve as fluorescent labeling probes for tracking the intracellular transport, while the GO combined with the aptamer conjugated on the outside of the nanocomposites facilitated the targeted drug delivery with enhanced loading capability.

Apart from drug delivery, graphene and its derivatives also show great potential in therapy. Owing to the low toxicity, low production costs, and strong optical absorbance in the NIR region of graphene and its derivatives, many applications combined therapy and bioimaging have been investigated recently.^{16, 71, 178-182} Chen and co-workers¹⁶¹ reported a novel, strongly fluorescent, nontoxic semiconductor quantum dots-

tagged reduced graphene oxide (QD-rGO) nanocomposite serving as an imaging agent in the visible-light region and a photothermal cancer therapy agent in the NIR region. Remarkably, the generated heat from the QD-rGO simultaneously caused a temperature increase and an obvious decrease in the QD brightness, which provided a mean for in situ heat/temperature sensing as well as photothermal therapy. Liu *et al.*¹⁸ prepared nanographene sheets (NGS) with PEG coating by a fluorescent labeling method. PEGylated NGS showed highly efficient tumor passive targeting and relatively low retention in reticuloendothelial systems. What's more, ultra efficient tumor ablation achieved after intravenous administration of NGS and low-power NIR laser irradiation on the tumor owing to the strong optical absorbance of NGS in the NIR region.

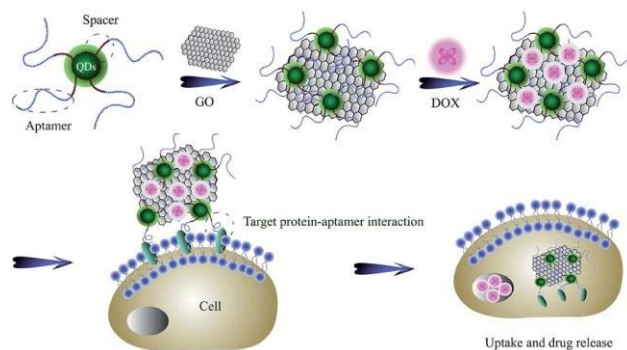


Fig. 7 Schematic presentation of the bio-imaging and cell-targeted drug delivery by using the aptamer-QD-GO nanocomposites. Copyright 2014 Royal Society of Chemistry.¹⁷⁷

CDs for bioimaging

As previously discussed, CDs have multiple advantages including comparable optical properties and good chemical and photochemical stability. CDs can not only be used for biosensing, but also may be an attractive candidate for bioimaging because of their excellent photoluminescence properties and low toxicity. Traditional QDs, such as CdTe and related core-shell nanoparticles, have been used variously in vitro and in vivo optical imaging experiments.¹⁸³⁻¹⁸⁵ However, the QDs contain toxic heavy metals, their application may bring health and environmental problems,¹⁸⁴ applying CDs for bioimaging has formed a trend. Moreover, because of the high photostability and biocompatibility, the CDs are also well suited for cellular imaging. For example, a fluorescent CDs-based, alternative, nontoxic imaging probe which is suitable for diagnostics was reported recently. These carbon nanoparticles were transformed into various functionalised nanoprobe as cell imaging probes with hydrodynamic diameters of 5–15 nm.¹⁸⁶ Li *et al.*¹⁸⁷ synthesized CDs with high yield (41.8%), high fluorescence QY (21.6%) and excellent stability in one simple step by carbonization of sucrose with oil acid. The obtained CDs can be well used for cell imaging. Nan *et al.*¹⁸⁸ used a simple and effective route employing lithium-intercalated graphite from lithium-ion batteries as a carbon source to prepare CDs. These CDs with water-soluble,

nanosized and biocompatible can easily enter into HeLa cells to act as a cell-imaging reagent without any further functionalization. Recently, Liu *et al.*¹⁸⁹ developed a simple hydrothermal approach to prepare the amorphous CDs with high two-photon fluorescence from hyperbranched poly(amino amine) and citric acid without further modification. The as-synthesized CDs exhibited excellent fluorescence properties and excitation-dependent fluorescence behavior with the corresponding QY of 17.1% in aqueous solution. Moreover, the CDs showed low cytotoxicity against L929 normal cells.

As fluorescence nanomaterials, CDs can delivery drugs with high loading efficiency as well as observe drugs distribution and monitor their effects.¹⁹⁰⁻¹⁹³ Chowdhury *et al.*¹⁹⁴ successfully prepared a novel carbon dot coated alginate beads (CA-CD) with peculiar stability and high loading efficiency in comparison to calcium alginate (CA) beads. Kim *et al.*¹⁹⁵ coupled CDs with gold nanoparticles for an assembly, which was then conjugated with polyethylenimine-plasmid DNA (pDNA) for delivering DNA to cells. The fluorescence emissions from the assembly of CD-gold nanoparticles could be quenched by pDNA while the release of pDNA could be probed by the recovery of the fluorescence signals. Sharon *et al.*¹⁹⁶ used phenylalanine derived non-toxic CDs as a vehicle for the delivery of anti-psychotic drug haloperidol (HaLO). Cysteamine hydrochloride (CysHCl) as a linker can offer controlled release under physiological conditions for more than 40 h following the Hixson–Crowell model under standardized conditions. Moreover, the CDs-CysHCl-HaLO conjugate was found to have a much higher compatibility with MDCK cells at pH 7.2 in comparison to bare HaLO.

As a kind of fluorescence nanomaterials, CDs also can combine medical therapy and bioimaging diagnostics for drug distribution visual and monitoring of their effects.^{191, 197} Sun *et al.*¹⁹⁸ prepared a multifunctional theranostic agent (CD-Oxa) by the conjugation of an anticancer agent (oxidized oxaliplatin, Oxa (IV) -COOH) on the surface of CDs (Fig. 8). CD-Oxa successfully combined the optical properties of CDs and the therapy performance of Oxa. In vitro, CD-Oxa performed good biocompatibility, bioimaging function, and anticancer effect. In vivo, the distribution of the drug can be monitored by the fluorescence signal of CD-Oxa.

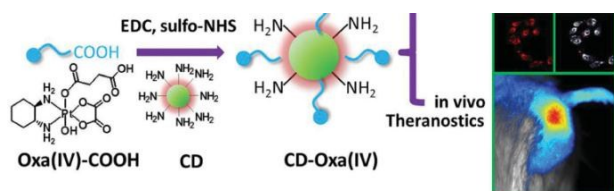


Fig. 8 Synthetic scheme for CD-Oxa and its applications in bioimaging and theranostics. Copyright 2014 Wiley-VCH.¹⁹⁸

Analogously, Zhou *et al.*¹⁹⁹ successfully synthesized multifunctional hybrid nanoparticles (NPs, ~100 nm) which combined magnetic Fe₃O₄ nanocrystals and CDs in porous carbon (C) via a one-pot solvothermal method by simply

increasing the H₂O₂ concentration. The mesoporous carbon shell and hydrophilic surface functional groups endowed the hybrid NPs with high loading capacity. Meanwhile, the Fe₃O₄@C-CDs hybrid NPs can absorb and convert NIR light to heat due to the existence of CDs, and thus, can realise NIR-controlled drug release and combined photothermal treatment for high therapeutic efficacy.

GQDs for bioimaging

Optical properties are the key of GQDs to be put into practical use. GQDs can be dissolved in most polar solvents without further chemical modifications and have high stability compared with other fluorescent dyes. So that GQDs can be used for bioimaging. Owing to bright PL, low cytotoxicity, excellent solubility and biocompatibility, GQDs are particularly eco-friendly and have been demonstrated to be excellent probes for bioimaging.^{133, 173, 200-203} Gong *et al.*²⁰⁴ demonstrated that nitrogen-doped graphene quantum dots (N-GQDs) were facilely prepared via a one-pot solvothermal approach using dimethyl formamide (DMF) as solvent and nitrogen source. The N-GQD exhibited a two-photon absorption cross section as high as 48 000 GM and were demonstrated as an efficient two-photon fluorescent probe for cellular and deep tissue imaging. Similarly, a one-step solvothermal method to prepare fluorescent GQDs for labeling and imaging cells was reported by Yang *et al.*⁴². Singh *et al.*²⁰⁰ reported a simple method for reducing the toxicity of GQDs by embedding them in PEG matrix. The enhanced biocompatibility of polymer modified GQDs can be used for the reduction of reactive oxygen species generation as well as cell imaging.

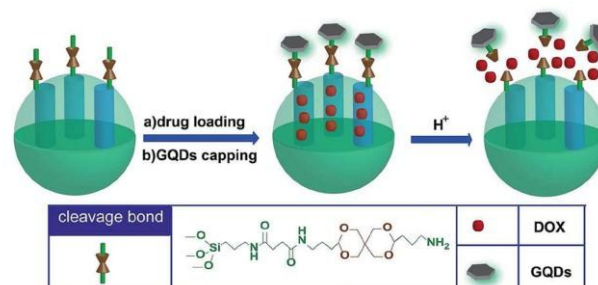


Fig. 9 Schematic representation of pH-triggered release of drug molecules from GQD-capped MSNs. Copyright 2014 Royal Society of Chemistry.²⁰⁸

GQDs could be used for loading cancer drugs through simple physical absorption via π - π stacking.^{203, 205-207} Contacting the excellent optical properties of GQDs, many applications have been made for bioimaging meanwhile delivering drug. For example, Nigam *et al.*²⁰³ applied hyaluronic acid and GQDs functionalized human serum albumin nanoparticles for bioimaging and targeted delivery of gemcitabine to pancreatic cancer. Gemcitabine, the most preferred drug for pancreatic cancer treatment, was encapsulated in albumin nanoparticles. Fu *et al.*²⁰⁸ designed a biocompatible pH-responsive drug delivery system by grafting GQDs on the surface of mesoporous silica nanoparticles (MSNs) via acid-cleavable

acetal bonds which could effectively prevent the leakage of drug molecules at neutral pH and release them at acidic pH (Fig. 9).

GQDs also can be applied in medical therapy. Like CDs, as a kind of fluorescence nanomaterials, GQDs can combine medical therapy and bioimaging. For example, Li *et al.*²⁰⁹ reported a one-step fabrication of multifunctional core-shell structured capsules using a coaxial electrospray method in order to achieve the integration of targeted therapy and bioimaging. The TiO₂ shell suppressed the initial burst release of paclitaxel while Fe₃O₄ and GQDs inside the oil core functioned successfully for magnetic targeting and fluorescence imaging, respectively. Moreover, depending on the intrinsic fluorescence properties, GQDs with ultra-small sizes and visible fluorescence emission have also been developed in recent years for applications in biomedical imaging. Guo *et al.*²¹⁰ successfully used GQDs to enhance nuclease activity of copper complexes. Owing to the efficient electron-transfer from the electron-rich GQDs to the copper complexes, GQDs promoted the reduction of copper ions and accelerated their reaction with O₂, forming superoxide anions and copper-centered radicals, which then oxidized DNA molecules. Recently, the development of GQDs as antibacterial agents develops quickly.²¹¹ Qu and co-workers²¹² reported an antibacterial system combining GQDs, with a low level of H₂O₂. They found that the peroxidase-like activity of GQDs originated from their ability to catalyze the decomposition of H₂O₂, generating ·OH. Since the ·OH had a higher antibacterial activity, the conversion of H₂O₂ into ·OH improved the antibacterial performance of H₂O₂, which made it possible to avoid the toxicity of H₂O₂ at high levels in wound disinfection. More importantly, GQDs-Band-Aids were prepared, which exhibited an excellent antibacterial feature in vivo when combining with a low concentration of H₂O₂, as illustrated in Fig. 10, indicating that GQDs-Band-Aids have promising applications for wound disinfection.

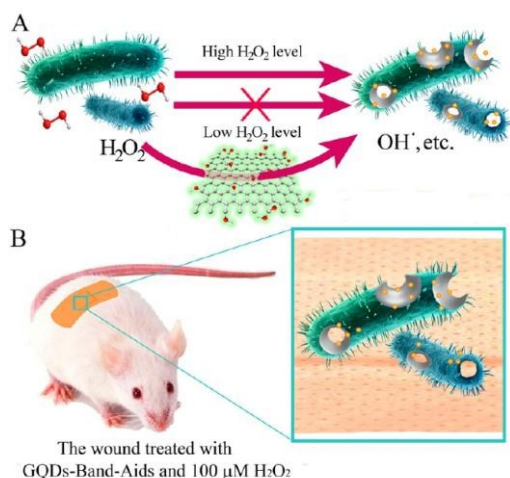


Fig. 10 (A) The designed system based on GQDs and low level of H₂O₂ for the antibacterial application. (B) The GQD Band-Aids used in wound disinfection in vivo. Copyright 2014 American Chemical Society.²¹²

Fullerene, CNHs and CNOs for bioimaging

There are also applications of fullerene, CNHs and CNOs for bioimaging in recent years. For example, Chen *et al.*²¹³ fabricated a composite nanofibrous material, consisting of fullerene nanoparticles and poly(L-lactide) by a simple electrospinning method which were successfully used as substrates for bioimaging in vitro. Xu *et al.*²¹⁴ synthesized a nanocomposite consisted of amino-modified NaYF₄:Yb,Er upconversion luminescent nanoparticles and single-walled CNHs via covalent linkage for the first time. The nanocomposite covalently coupled with rabbit anti-CEA8 antibody was successfully used as a cell labeling agent for the immunolabeling and imaging of HeLa cells. Sarkar and co-workers²¹⁵ successfully used water-soluble CNOs as highly-fluorescent bioimaging agent for in common food web of two model organisms: unicellular *Escherichia coli* (*E. coli*) and multicellular *Caenorhabditis elegans* (*C. elegans*) with no toxic effect.

Summary and outlook

The past five years have witnessed the tremendous development of carbon materials. They are extensively used for various biological applications including fluorescence biosensing and bioimaging. This review article mainly focuses on the modifications as well as fluorescence biosensing and bioimaging applications of carbon nanomaterials such as carbon nanotubes, graphene, carbon dots, graphene quantum dots, fullerene, CNHs and CNOs. Furthermore, the modifications of these carbon nanomaterials are widely used for better applications of fluorescence biosensors, imaging probes and so on. Also, conjugating various targeting molecules, drugs, genes and contrast agents to carbon nanomaterials is widely investigated in the bioimaging and treatment of cancer cells and tumors. Biological applications of carbon nanomaterials are significantly impacting current biotechnology. Especially, the carbon nanomaterials enable the development of biosensors with enhanced sensitivity, better selectivity and a wide range of detection. Multiple-detection has also been achieved with a low LOD and a high sensitivity. The biocompatible properties of carbon nanomaterials make them applicable for in situ detection of living cells.

In summary, carbon nanomaterials have proven themselves as highly promising fluorescence biosensing and bioimaging tools. In order to realize their more enormously biosensing and bioimaging applications combined diagnosis and therapy, it is important to appropriately control and tune the size, shape, morphology and surface modifications of carbon nanomaterials to satisfy requirements of high biocompatibility, long-time stability and accurate targeting ability in vivo. The current research suggests that carbon nanomaterials have a promising outlook for various biological applications.

Acknowledgements

The authors acknowledge the Scientific Research Foundation of Northwest A&F University (Z111021103 and Z111021107), the National Natural Science Foundation of China (No. 21206137, 21272030, 201205095), the Open Project Program of Key Laboratory of ECO-Textiles (Jiangnan University), the Ministry of Education (No. KLET1102), Shaanxi Province Science and Technology (No. 2013K12-03-23), State Key Laboratory of Chemo/Biosensing and Chemometrics, Hunan University (No. 2013005).

Notes and references

- S. Iijima and T. Ichihashi, *Nature*, 1993, **363**, 603-605.
- P. M. Ajayan and S. Iijima, *Nature*, 1992, **358**, 23-23.
- B. Q. Wei, R. Vajtai, Y. Jung, J. Ward, R. Zhang, G. Ramanath and P. M. Ajayan, *Nature*, 2002, **416**, 495-496.
- X. H. Peng, J. Y. Chen, J. A. Misewich and S. S. Wong, *Chem. Soc. Rev.*, 2009, **38**, 1076-1098.
- N. M. Bandaru and N. H. Voelcker, *J. Mater. Chem.*, 2012, **22**, 8748-8758.
- Z. A. Liu, K. Yang and S. T. Lee, *J. Mater. Chem.*, 2011, **21**, 586-598.
- X. M. Li, X. Liu, J. Huang, Y. B. Fan and F. Z. Cui, *Surf. Coat. Technol.*, 2011, **206**, 759-766.
- S. Y. Madani, N. Naderi, O. Dissanayake, A. Tan and A. M. Seifalian, *Int. J. Nanomed.*, 2011, **6**, 2963-2979.
- K. S. Novoselov, A. K. Geim, S. V. Morozov, D. Jiang, Y. Zhang, S. V. Dubonos, I. V. Grigorieva and A. A. Firsov, *Science*, 2004, **306**, 666-669.
- X. Huang, Z. Y. Yin, S. X. Wu, X. Y. Qi, Q. Y. He, Q. C. Zhang, Q. Y. Yan, F. Boey and H. Zhang, *Small*, 2011, **7**, 1876-1902.
- M. Pumera, *Chem. Soc. Rev.*, 2010, **39**, 4146-4157.
- Y. Zhang, T. R. Nayak, H. Hong and W. B. Cai, *Nanoscale*, 2012, **4**, 3833-3842.
- L. Z. Feng and Z. A. Liu, *Nanomedicine*, 2011, **6**, 317-324.
- K. Yang, J. M. Wan, S. Zhang, B. Tian, Y. J. Zhang and Z. Liu, *Biomaterials*, 2012, **33**, 2206-2214.
- K. Yang, L. L. Hu, X. X. Ma, S. Q. Ye, L. Cheng, X. Z. Shi, C. H. Li, Y. G. Li and Z. Liu, *Adv. Mater.*, 2012, **24**, 1868-1872.
- B. Tian, C. Wang, S. Zhang, L. Z. Feng and Z. Liu, *Acs Nano*, 2011, **5**, 7000-7009.
- S. A. Zhang, K. Yang, L. Z. Feng and Z. Liu, *Carbon*, 2011, **49**, 4040-4049.
- K. Yang, S. A. Zhang, G. X. Zhang, X. M. Sun, S. T. Lee and Z. A. Liu, *Nano Lett.*, 2010, **10**, 3318-3323.
- H. Shen, L. M. Zhang, M. Liu and Z. J. Zhang, *Theranostics*, 2012, **2**, 283-294.
- S. J. He, B. Song, D. Li, C. F. Zhu, W. P. Qi, Y. Q. Wen, L. H. Wang, S. P. Song, H. P. Fang and C. H. Fan, *Adv. Funct. Mater.*, 2010, **20**, 453-459.
- L. A. L. Tang, J. Z. Wang and K. P. Loh, *J. Am. Chem. Soc.*, 2010, **132**, 10976-10977.
- L. M. Zhang, J. G. Xia, Q. H. Zhao, L. W. Liu and Z. J. Zhang, *Small*, 2010, **6**, 537-544.
- L. M. Zhang, Z. X. Lu, Q. H. Zhao, J. Huang, H. Shen and Z. J. Zhang, *Small*, 2011, **7**, 460-464.
- P. C. Hsu, Z. Y. Shih, C. H. Lee and H. T. Chang, *Green Chem.*, 2012, **14**, 917-920.
- S. Chandra, S. H. Pathan, S. Mitra, B. H. Modha, A. Goswami and P. Pramanik, *Rsc Adv.*, 2012, **2**, 3602-3606.
- M. M. Liu and W. Chen, *Nanoscale*, 2013, **5**, 12558-12564.
- S. N. Baker and G. A. Baker, *Angew. Chem. Int. Ed.*, 2010, **49**, 6726-6744.
- X. Y. Xu, R. Ray, Y. L. Gu, H. J. Ploehn, L. Gearheart, K. Raker and W. A. Scrivens, *J. Am. Chem. Soc.*, 2004, **126**, 12736-12737.
- W. Kwon, G. Lee, S. Do, T. Joo and S. W. Rhee, *Small*, 2014, **10**, 506-513.
- C. Yuan, B. H. Liu, F. Liu, M. Y. Han and Z. P. Zhang, *Anal. Chem.*, 2014, **86**, 1123-1130.
- J. Tang, B. Kong, H. Wu, M. Xu, Y. C. Wang, Y. L. Wang, D. Y. Zhao and G. F. Zheng, *Adv. Mater.*, 2013, **25**, 6569-6574.
- A. L. Antaris, J. T. Robinson, O. K. Yaghi, G. S. Hong, S. Diao, R. Luong and H. J. Dai, *Acs Nano*, 2013, **7**, 3644-3652.
- J. H. Li, G. Wang, H. Q. Zhu, M. Zhang, X. H. Zheng, Z. F. Di, X. Y. Liu and X. Wang, *Sci. Rep-UK*, 2014, **4**, DOI: 10.1038/srep04359.
- A. Kleinauskas, S. Rocha, S. Sahu, Y. P. Sun and P. Juzenas, *Nanotechnology*, 2013, **24**, DOI: 10.1088/0957-4484/24/32/325103.
- Y. S. Liu, Y. A. Zhao and Y. Y. Zhang, *Sensor Actuat. B-chem*, 2014, **196**, 647-652.
- S. Chandra, P. Das, S. Bag, D. Laha and P. Pramanik, *Nanoscale*, 2011, **3**, 1533-1540.
- L. B. Tang, R. B. Ji, X. K. Cao, J. Y. Lin, H. X. Jiang, X. M. Li, K. S. Teng, C. M. Luk, S. J. Zeng, J. H. Hao and S. P. Lau, *Acs Nano*, 2012, **6**, 5102-5110.
- S. J. Zhuo, M. W. Shao and S. T. Lee, *Acs Nano*, 2012, **6**, 1059-1064.
- S. J. Zhu, J. H. Zhang, S. J. Tang, C. Y. Qiao, L. Wang, H. Y. Wang, X. Liu, B. Li, Y. F. Li, W. L. Yu, X. F. Wang, H. C. Sun and B. Yang, *Adv. Funct. Mater.*, 2012, **22**, 4732-4740.
- H. Razmi and R. Mohammad-Rezaei, *Biosens. Bioelectron.*, 2013, **41**, 498-504.
- H. M. Zhao, Y. Y. Chang, M. Liu, S. Gao, H. T. Yu and X. Quan, *Chem. Commun.*, 2013, **49**, 234-236.
- S. J. Zhu, J. H. Zhang, C. Y. Qiao, S. J. Tang, Y. F. Li, W. J. Yuan, B. Li, L. Tian, F. Liu, R. Hu, H. N. Gao, H. T. Wei, H. Zhang, H. C. Sun and B. Yang, *Chem. Commun.*, 2011, **47**, 6858-6860.
- Y. Q. Dong, C. Q. Chen, X. T. Zheng, L. L. Gao, Z. M. Cui, H. B. Yang, C. X. Guo, Y. W. Chi and C. M. Li, *J. Mater. Chem.*, 2012, **22**, 8764-8766.
- V. Gupta, N. Chaudhary, R. Srivastava, G. D. Sharma, R. Bhardwaj and S. Chand, *J. Am. Chem. Soc.*, 2011, **133**, 9960-9963.
- D. Jariwala, V. K. Sangwan, L. J. Lauhon, T. J. Marks and M. C. Hersam, *Chem. Soc. Rev.*, 2013, **42**, 2824-2860.
- S. Iijima, M. Yudasaka, R. Yamada, S. Bandow, K. Suenaga, F. Kokai and K. Takahashi, *Chem. Phys. Lett.*, 1999, **309**, 165-170.
- D. Ugarte, *Nature*, 1992, **359**, 707-709.
- K. Kostarelos, A. Bianco and M. Prato, *Nat. Nanotechnol.*, 2009, **4**, 627-633.
- J. H. Shen, Y. H. Zhu, X. L. Yang and C. Z. Li, *Chem. Commun.*, 2012, **48**, 3686-3699.
- H. T. Li, X. D. He, Y. Liu, H. Huang, S. Y. Lian, S. T. Lee and Z. H. Kang, *Carbon*, 2011, **49**, 605-609.
- Q. Li, T. Y. Ohulchanskyy, R. L. Liu, K. Koynov, D. Q. Wu, A. Best, R. Kumar, A. Bonoiu and P. N. Prasad, *J. Phys. Chem. C*, 2010, **114**, 12062-12068.
- D. Y. Pan, L. Guo, J. C. Zhang, C. Xi, Q. Xue, H. Huang, J. H. Li, Z. W. Zhang, W. J. Yu, Z. W. Chen, Z. Li and M. H. Wu, *J. Mater. Chem.*, 2012, **22**, 3314-3318.
- B. C. Thompson, J. Chen, S. E. Moulton and G. G. Wallace, *Nanoscale*, 2010, **2**, 499-501.
- Y. L. Zhao and J. F. Stoddart, *Acc Chem. Res.*, 2009, **42**, 1161-1171.
- Y. Liu, X. Dong and P. Chen, *Chem. Soc. Rev.*, 2012, **41**, 2283-2307.
- Y. F. Wang and A. G. Hu, *J. Mater. Chem. C*, 2014, **2**, 6921-6939.
- L. L. Li, G. H. Wu, G. H. Yang, J. Peng, J. W. Zhao and J. J. Zhu, *Nanoscale*, 2013, **5**, 4015-4039.
- H. C. Wu, X. L. Chang, L. Liu, F. Zhao and Y. L. Zhao, *J. Mater. Chem.*, 2010, **20**, 1036-1052.
- J. Liu, A. G. Rinzler, H. J. Dai, J. H. Hafner, R. K. Bradley, P. J. Boul, A. Lu, T. Iversen, K. Shelimov, C. B. Huffman, F. Rodriguez-Macias, Y. S. Shon, T. R. Lee, D. T. Colbert and R. E. Smalley, *Science*, 1998, **280**, 1253-1256.
- L. H. Liu, M. M. Lerner and M. D. Yan, *Nano Lett.*, 2010, **10**, 3754-3756.
- Y. H. Yang, J. H. Cui, M. T. Zheng, C. F. Hu, S. Z. Tan, Y. Xiao, Q. Yang and Y. L. Liu, *Chem. Commun.*, 2012, **48**, 380-382.
- S. N. Qu, X. Y. Wang, Q. P. Lu, X. Y. Liu and L. J. Wang, *Angew. Chem. Int. Ed.*, 2012, **51**, 12215-12218.
- H. T. Li, Z. H. Kang, Y. Liu and S. T. Lee, *J. Mater. Chem.*, 2012, **22**,

- 24230-24253.
64. H. T. Li, R. H. Liu, Y. Liu, H. Huang, H. Yu, H. Ming, S. Y. Lian, S. T. Lee and Z. H. Kang, *J. Mater. Chem.*, 2012, **22**, 17470-17475.
65. X. J. Zhou, Y. Zhang, C. Wang, X. C. Wu, Y. Q. Yang, B. Zheng, H. X. Wu, S. W. Guo and J. Y. Zhang, *ACS Nano*, 2012, **6**, 6592-6599.
66. E. J. Wallace, R. S. G. D'Rozario, B. M. Sanchez and M. S. P. Sansom, *Nanoscale*, 2010, **2**, 967-975.
67. Y. X. Huang, X. C. Dong, Y. M. Shi, C. M. Li, L. J. Li and P. Chen, *Nanoscale*, 2010, **2**, 1485-1488.
68. X. C. Dong, W. Huang and P. Chen, *Nanoscale Res. Lett.*, 2011, **6**, DOI: 10.1007/s11671-010-9806-8.
69. S. Mao, G. H. Lu, K. H. Yu, Z. Bo and J. H. Chen, *Adv. Mater.*, 2010, **22**, 3521-3526.
70. S. Park, N. Mohanty, J. W. Suk, A. Nagaraja, J. H. An, R. D. Piner, W. W. Cai, D. R. Dreyer, V. Berry and R. S. Ruoff, *Adv. Mater.*, 2010, **22**, 1736-1740.
71. J. T. Robinson, S. M. Tabakman, Y. Y. Liang, H. L. Wang, H. S. Casalongue, D. Vinh and H. J. Dai, *J. Am. Chem. Soc.*, 2011, **133**, 6825-6831.
72. H. F. Dong, L. Ding, F. Yan, H. X. Ji and H. X. Ju, *Biomaterials*, 2011, **32**, 3875-3882.
73. W. B. Hu, C. Peng, M. Lv, X. M. Li, Y. J. Zhang, N. Chen, C. H. Fan and Q. Huang, *ACS Nano*, 2011, **5**, 3693-3700.
74. K. P. Liu, J. J. Zhang, F. F. Cheng, T. T. Zheng, C. M. Wang and J. J. Zhu, *J. Mater. Chem.*, 2011, **21**, 12034-12040.
75. E. Dubuisson, Z. Y. Yang and K. P. Loh, *Anal. Chem.*, 2011, **83**, 2452-2460.
76. Z. Y. Yin, Q. Y. He, X. Huang, J. Zhang, S. X. Wu, P. Chen, G. Lu, P. Chen, Q. C. Zhang, Q. Y. Yan and H. Zhang, *Nanoscale*, 2012, **4**, 293-297.
77. H. L. Li, Y. W. Zhang, L. Wang, J. Q. Tian and X. P. Sun, *Chem. Commun.*, 2011, **47**, 961-963.
78. Z. Zhu, R. H. Yang, M. X. You, X. L. Zhang, Y. R. Wu and W. H. Tan, *Analytical and Bioanalytical Chemistry*, 2010, **396**, 73-83.
79. Y. Huang, S. L. Zhao, Y. M. Liu, J. Chen, Z. F. Chen, M. Shi and H. Liang, *Chem. Commun.*, 2012, **48**, 9400-9402.
80. Y. Meng, F. Y. Liu, J. F. Han, S. G. Sun, J. L. Fan, F. L. Song and X. J. Peng, *Materials Science and Engineering B-Advanced Functional Solid-State Materials*, 2012, **177**, 887-891.
81. W. Wang, L. Zhan, Y. Q. Du, F. Leng, Y. Chang, M. X. Gao and C. Z. Huang, *Anal. Methods-UK*, 2013, **5**, 5555-5559.
82. K. Nam, K. Eom, J. Yang, J. Park, G. Lee, K. Jang, H. Lee, S. W. Lee, D. S. Yoon, C. Y. Lee and T. Kwon, *J. Mater. Chem.*, 2012, **22**, 23348-23356.
83. Y. Iizumi, T. Okazaki, Y. Ikehara, M. Ogura, S. Fukata and M. Yudasaka, *ACS Appl. Mater. Interfaces*, 2013, **5**, 7665-7670.
84. T. Bhattacharyya, S. Samaddar and A. K. Dasgupta, *Nanoscale*, 2013, **5**, 9231-9237.
85. J. Q. Zhang, A. A. Boghossian, P. W. Barone, A. Rwei, J. H. Kim, D. H. Lin, D. A. Heller, A. J. Hilmer, N. Nair, N. F. Reuel and M. S. Strano, *J. Am. Chem. Soc.*, 2011, **133**, 567-581.
86. Y. He, G. M. Huang and H. Cui, *ACS Appl. Mater. Interfaces*, 2013, **5**, 11336-11340.
87. S. Guo, D. X. Du, L. N. Tang, Y. Ning, Q. F. Yao and G. J. Zhang, *Analyst*, 2013, **138**, 3216-3220.
88. W. Zhang, F. H. Li, Y. W. Hu, S. Y. Gan, D. X. Han, Q. X. Zhang and L. Niu, *J. Mater. Chem. B*, 2014, **2**, 3142-3148.
89. Y. H. Lin, Y. Tao, F. Pu, J. S. Ren and X. G. Qu, *Adv. Funct. Mater.*, 2011, **21**, 4565-4572.
90. Z. W. Tang, H. Wu, J. R. Cort, G. W. Buchko, Y. Y. Zhang, Y. Y. Shao, I. A. Aksay, J. Liu and Y. H. Lin, *Small*, 2010, **6**, 1205-1209.
91. H. S. Jeong, M. Park, J. W. Yi, T. Joo and B. H. Kim, *Mol. Biosyst.*, 2010, **6**, 951-953.
92. C. H. Lu, J. Li, J. J. Liu, H. H. Yang, X. Chen and G. N. Chen, *Chem.-Eur. J.*, 2010, **16**, 4889-4894.
93. H. J. Li, J. Wen, R. J. Yu, J. Meng, C. Wang, C. X. Wang and S. G. Sun, *RSC Adv.*, 2015, **5**, 9341-9347.
94. Y. Tao, Y. H. Lin, Z. Z. Huang, J. S. Ren and X. G. Qu, *Analyst*, 2012, **137**, 2588-2592.
95. H. J. Li, F. Y. Liu, J. F. Han, M. Z. Cai, S. G. Sun, J. L. Fan, F. L. Song and X. J. Peng, *J. Mater. Chem. B*, 2013, **1**, 693-697.
96. H. L. Zhuang, S. J. Zhen, J. Wang and C. Z. Huang, *Anal. Methods-UK*, 2013, **5**, 208-212.
97. S. J. Zhen, H. L. Zhuang, J. Wang and C. Z. Huang, *Anal. Methods-UK*, 2013, **5**, 6904-6907.
98. J. Zhou, X. H. Xu, W. Liu, X. Liu, Z. Nie, M. Qing, L. H. Nie and S. Z. Yao, *Anal. Chem.*, 2013, **85**, 5746-5754.
99. M. Liu, J. P. Song, S. M. Shuang, C. Dong, J. D. Brennan and Y. F. Li, *ACS Nano*, 2014, **8**, 5564-5573.
100. G. L. Wang, X. F. Xu, X. M. Wu, G. X. Cao, Y. M. Dong and Z. J. Li, *J. Phys. Chem. C*, 2014, **118**, 28109-28117.
101. A. Mondal and N. R. Jana, *Chem. Commun.*, 2012, **48**, 7316-7318.
102. Z. S. Qian, J. J. Ma, X. Y. Shan, H. Feng, L. X. Shao and J. R. Chen, *Chem.-Eur. J.*, 2014, **20**, 2254-2263.
103. X. M. Lin, G. M. Gao, L. Y. Zheng, Y. W. Chi and G. N. Chen, *Anal. Chem.*, 2014, **86**, 1223-1228.
104. X. J. Liu, N. Zhang, T. Bing and D. H. Shangguan, *Anal. Chem.*, 2014, **86**, 2289-2296.
105. F. K. Du, F. Zeng, Y. H. Ming and S. Z. Wu, *Microchim. Acta*, 2013, **180**, 453-460.
106. R. X. Wang, G. L. Li, Y. Q. Dong, Y. W. Chi and G. N. Chen, *Anal. Chem.*, 2013, **85**, 8065-8069.
107. A. Cayuela, M. L. Soriano and M. Valcarcel, *Anal. Chim. Acta*, 2013, **804**, 246-251.
108. Y. Q. Dong, C. Q. Chen, J. P. Lin, N. N. Zhou, Y. W. Chi and G. N. Chen, *Carbon*, 2013, **56**, 12-17.
109. J. X. Shi, C. Lu, D. Yan and L. N. Ma, *Biosens. Bioelectron.*, 2013, **45**, 58-64.
110. J. Z. Li, N. Y. Wang, T. T. Tran, C. A. Huang, L. Chen, L. J. Yuan, L. P. Zhou, R. Shen and Q. Y. Cai, *Analyst*, 2013, **138**, 2038-2043.
111. J. J. Niu and H. Gao, *J. Lumin.*, 2014, **149**, 159-162.
112. Q. T. Huang, S. R. Hu, H. Q. Zhang, J. H. Chen, Y. S. He, F. M. Li, W. Weng, J. C. Ni, X. X. Bao and Y. Lin, *Analyst*, 2013, **138**, 5417-5423.
113. M. Zheng, Z. G. Xie, D. Qu, D. Li, P. Du, X. B. Jing and Z. C. Sun, *ACS Appl. Mater. Interfaces*, 2013, **5**, 13242-13247.
114. Y. Mao, Y. Bao, D. X. Han, F. H. Li and L. Niu, *Biosens. Bioelectron.*, 2012, **38**, 55-60.
115. L. Zhou, Y. H. Lin, Z. Z. Huang, J. S. Ren and X. G. Qu, *Chem. Commun.*, 2012, **48**, 1147-1149.
116. K. G. Qu, J. S. Wang, J. S. Ren and X. G. Qu, *Chem.-Eur. J.*, 2013, **19**, 7243-7249.
117. E. H. Noh, H. Y. Ko, C. H. Lee, M. S. Jeong, Y. W. Chang and S. Kim, *J. Mater. Chem. B*, 2013, **1**, 4438-4445.
118. B. L. Xu, C. Q. Zhao, W. L. Wei, J. S. Ren, D. Miyoshi, N. Sugimoto and X. G. Qu, *Analyst*, 2012, **137**, 5483-5486.
119. S. Maiti, K. Das and P. K. Das, *Chem. Commun.*, 2013, **49**, 8851-8853.
120. S. Kiran and R. Misra, *Mater. Technol.: Adv. Perform. Mater.*, 2014, DOI: <http://dx.doi.org/10.1179/1753555714Y.0000000257>.
121. J. J. Lu, M. Yan, L. Ge, S. G. Ge, S. W. Wang, J. X. Yan and J. H. Yu, *Biosens. Bioelectron.*, 2013, **47**, 271-277.
122. I. Al-Ogaidi, H. L. Gou, Z. P. Aguilar, S. W. Guo, A. K. Melconian, A. K. A. Al-Kazaz, F. K. Meng and N. Q. Wu, *Chem. Commun.*, 2014, **50**, 1344-1346.
123. Y. Wang, L. Zhang, R. P. Liang, J. M. Bai and J. D. Qiu, *Anal. Chem.*, 2013, **85**, 9148-9155.
124. Sandra Benítez-Martínez, A. n. I. L. pez-Lorente and M. V. rcel, *Anal. Chem.*, 2014, **86**, 12279-12284.
125. L. Wang, J. Zheng, Y. Li, S. Yang, C. Liu, Y. Xiao, J. Li, Z. Cao and R. Yang, *Anal. Chem.*, 2014.
126. X. Ran, H. J. Sun, F. Pu, J. S. Ren and X. G. Qu, *Chem. Commun.*, 2013, **49**, 1079-1081.
127. L. L. Li, J. Ji, R. Fei, C. Z. Wang, Q. Lu, J. R. Zhang, L. P. Jiang and J. J. Zhu, *Adv. Funct. Mater.*, 2012, **22**, 2971-2979.
128. Y. Zhou, Z. B. Qu, Y. B. Zeng, T. S. Zhou and G. Y. Shi, *Biosens. Bioelectron.*, 2014, **52**, 317-323.
129. F. X. Wang, Z. Y. Gu, W. Lei, W. J. Wang, X. F. Xia and Q. L. Hao, *Sensor Actuat. B-chem*, 2014, **190**, 516-522.
130. J. Ju and W. Chen, *Biosens. Bioelectron.*, 2014, **58**, 219-225.

131. H. J. Sun, L. Wu, W. L. Wei and X. G. Qu, *Mater. Today*, 2013, **16**, 433-442.
132. Z. S. Qian, X. Y. Shan, L. J. Chai, J. J. Ma, J. R. Chen and H. Feng, *Nanoscale*, 2014, **6**, 5671-5674.
133. J. Ju, R. Z. Zhang, S. J. He and W. Chen, *Rsc Adv.*, 2014, **4**, 52583-52589.
134. Z. Z. Wu, W. Y. Li, J. Chen and C. Yu, *Talanta*, 2014, **119**, 538-543.
135. L. L. Wang, J. Zheng, Y. H. Li, S. Yang, C. H. Liu, Y. Xiao, J. S. Li, Z. Cao and R. H. Yang, *Anal. Chem.*, 2014, **86**, 12348-12354.
136. X. J. Liu, I. Marangon, G. Melinte, C. Wilhelm, C. Menard-Moyon, B. P. Pichon, O. Ersen, K. Aubertin, W. Baaziz, C. Pham-Huu, S. Begin-Colin, A. Bianco, F. Gazeau and D. Begin, *Acs Nano*, 2014, **8**, 11290-11304.
137. H. Gong, R. Peng and Z. Liu, *Adv. Drug Delivery Rev.*, 2013, **65**, 1951-1963.
138. D. Ag, M. Selec, R. Bongartz, M. Can, S. Yurteri, I. Cianga, F. Stahl, S. Timur, T. Scheper and Y. Yagci, *Biomacromolecules*, 2013, **14**, 3532-3541.
139. R. El-Sayed, M. Eita, A. Barrefelt, F. Ye, H. Jain, M. Fares, A. Lundin, M. Crona, K. Abu-Salah, M. Muhammed and M. Hassan, *Nano Lett.*, 2013, **13**, 1393-1398.
140. J. J. Khandare, A. Jalota-Badhwari, S. D. Satavalekar, S. G. Bhansali, N. D. Aher, F. Kharas and S. S. Banerjee, *Nanoscale*, 2012, **4**, 837-844.
141. P. Bajaj, C. Mikoryak, R. H. Wang, D. K. Bushdiecker, P. Memon, R. K. Draper, G. R. Dieckmann, P. Pantano and I. H. Musselman, *Analyst*, 2014, **139**, 3069-3076.
142. Y. Liu, J. Huang, M. J. Sun, J. C. Yu, Y. L. Chen, Y. Q. Zhang, S. J. Jiang and Q. D. Shen, *Nanoscale*, 2014, **6**, 1480-1489.
143. B. D. Chen, H. Zhang, C. X. Zhai, N. Du, C. Sun, J. W. Xue, D. R. Yang, H. Huang, B. Zhang, Q. P. Xie and Y. L. Wu, *J. Mater. Chem.*, 2010, **20**, 9895-9902.
144. L. Minati, V. Antonini, M. Dalla Serra and G. Speranza, *Langmuir*, 2012, **28**, 15900-15906.
145. S. R. Datir, M. Das, R. P. Singh and S. Jain, *Bioconjugate Chem.*, 2012, **23**, 2201-2213.
146. Y. X. Wang, S. T. Yang, Y. L. Wang, Y. F. Liu and H. F. Wang, *Colloids Surf. B*, 2012, **97**, 62-69.
147. B. S. Wong, S. L. Yoong, A. Jagusiak, T. Panczyk, H. K. Ho, W. H. Ang and G. Pastorin, *Adv. Drug Delivery Rev.*, 2013, **65**, 1964-2015.
148. P. Liu, *Ind. Eng. Chem. Res.*, 2013, **52**, 13517-13527.
149. K. S. Siu, X. F. Zheng, Y. L. Liu, Y. J. Zhang, X. S. Zhang, D. Chen, K. Yuan, E. R. Gillies, J. Koropatnick and W. P. Min, *Bioconjugate Chem.*, 2014, **25**, 1744-1751.
150. T. Anderson, R. Hu, C. B. Yang, H. S. Yoon and K. T. Yong, *Biomater. Sci.*, 2014, **2**, 1244-1253.
151. C. Wang, C. C. Bao, S. J. Liang, H. L. Fu, K. Wang, M. Deng, Q. D. Liao and D. X. Cui, *Nanoscale Res. Lett.*, 2014, **9**, DOI: 10.1186/1556-276X-9-264.
152. A. de la Zerda, S. Bodapati, R. Teed, S. Y. May, S. M. Tabakman, Z. Liu, B. T. Khuri-Yakub, X. Y. Chen, H. J. Dai and S. S. Gambhir, *Acs Nano*, 2012, **6**, 4694-4701.
153. K. Yang, L. Z. Feng, X. Z. Shi and Z. Liu, *Chem. Soc. Rev.*, 2013, **42**, 530-547.
154. M. Nurunnabi, Z. Khatun, G. R. Reeck, D. Y. Lee and Y. K. Lee, *Chem. Commun.*, 2013, **49**, 5079-5081.
155. S. X. Shi, F. Chen, E. B. Ehlerding and W. B. Cai, *Bioconjugate Chem.*, 2014, **25**, 1609-1619.
156. M. Nurunnabi, Z. Khatun, G. R. Reeck, D. Y. Lee and Y. K. Lee, *Acs Appl. Mater. Interfaces*, 2014, **6**, 12413-12421.
157. M. X. Zhang, Y. H. Cao, Y. Chong, Y. F. Ma, H. L. Zhang, Z. W. Deng, C. H. Hu and Z. J. Zhang, *Acs Appl. Mater. Interfaces*, 2013, **5**, 13325-13332.
158. W. H. Chen, P. W. Yi, Y. Zhang, L. M. Zhang, Z. W. Deng and Z. J. Zhang, *Acs Appl. Mater. Interfaces*, 2011, **3**, 4085-4091.
159. H. J. Li, F. Y. Liu, S. G. Sun, J. Y. Wang, Z. Y. Li, D. Z. Mu, B. Qiao and X. J. Peng, *J. Mater. Chem. B*, 2013, **1**, 4146-4151.
160. F. Y. Liu, Y. L. Gao, H. J. Li and S. G. Sun, *Carbon*, 2014, **71**, 190-195.
161. S. H. Hu, Y. W. Chen, W. T. Hung, I. W. Chen and S. Y. Chen, *Adv. Mater.*, 2012, **24**, 1748-1754.
162. C. S. Wang, J. Y. Li, C. Amatore, Y. Chen, H. Jiang and X. M. Wang, *Angew. Chem. Int. Ed.*, 2011, **50**, 11644-11648.
163. Y. Sheng, X. S. Tang, E. W. Peng and J. M. Xue, *J. Mater. Chem. B*, 2013, **1**, 512-521.
164. X. Y. Yang, Y. S. Wang, X. Huang, Y. F. Ma, Y. Huang, R. C. Yang, H. Q. Duan and Y. S. Chen, *J. Mater. Chem.*, 2011, **21**, 3448-3454.
165. R. Justin and B. Q. Chen, *J. Mater. Chem. B*, 2014, **2**, 3759-3770.
166. T. Kavitha, S. I. H. Abdi and S. Y. Park, *Phys. Chem. Chem. Phys.*, 2013, **15**, 5176-5185.
167. F. F. Cheng, W. Chen, L. H. Hu, G. Chen, H. T. Miao, C. Z. Li and J. J. Zhu, *J. Mater. Chem. B*, 2013, **1**, 4956-4962.
168. Y. N. Ni, F. Y. Zhang and S. Kokot, *Anal. Chim. Acta*, 2013, **769**, 40-48.
169. H. L. Hu, C. Tang and C. H. Yin, *Mater. Lett.*, 2014, **125**, 82-85.
170. W. Miao, G. Shim, C. M. Kang, S. Lee, Y. S. Choe, H. G. Choi and Y. K. Oh, *Biomaterials*, 2013, **34**, 9638-9647.
171. G. Shim, J. Y. Kim, J. Han, S. W. Chung, S. Lee, Y. Byun and Y. K. Oh, *J. Controlled Release*, 2014, **189**, 80-89.
172. J. Q. Chen, H. Y. Liu, C. B. Zhao, G. Q. Qin, G. N. Xi, T. Li, X. P. Wang and T. S. Chen, *Biomaterials*, 2014, **35**, 4986-4995.
173. X. J. Wang, X. Sun, J. Lao, H. He, T. T. Cheng, M. Q. Wang, S. J. Wang and F. Huang, *Colloids Surf. B*, 2014, **122**, 638-644.
174. C. L. Weaver, J. M. LaRosa, X. L. Luo and X. T. Cui, *Acs Nano*, 2014, **8**, 1834-1843.
175. X. Ma, Q. Y. Qu, Y. Zhao, Z. Luo, Y. Zhao, K. W. Ng and Y. L. Zhao, *J. Mater. Chem. B*, 2013, **1**, 6495-6500.
176. R. Y. Zhang, M. Hummelgard, G. Lv and H. Olin, *Carbon*, 2011, **49**, 1126-1132.
177. L. Zhang, S. J. Xiao, L. L. Zheng, Y. F. Li and C. Z. Huang, *J. Mater. Chem. B*, 2014, **2**, 8558-8565.
178. J. L. Li, X. L. Hou, H. C. Bao, L. Sun, B. Tang, J. F. Wang, X. G. Wang and M. Gu, *J. Biomed. Mater. Res. A*, 2014, **102**, 2181-2188.
179. O. Akhavan, E. Ghaderi, S. Aghayee, Y. Fereydooni and A. Talebi, *J. Mater. Chem.*, 2012, **22**, 13773-13781.
180. O. Akhavan, E. Ghaderi and H. Emamy, *J. Mater. Chem.*, 2012, **22**, 20626-20633.
181. X. W. Zheng, W. H. Chen, P. Cui, Z. M. Wang and W. Zhang, *Rsc Adv.*, 2014, **4**, 58489-58494.
182. G. Gollavelli and Y. C. Ling, *Biomaterials*, 2014, **35**, 4499-4507.
183. X. H. Gao, L. L. Yang, J. A. Petros, F. F. Marshal, J. W. Simons and S. M. Nie, *Curr. Opin. Biotechnol.*, 2005, **16**, 63-72.
184. R. Hardman, *Environ. Health Persp.*, 2006, **114**, 165-172.
185. J. K. Jaiswal and S. M. Simon, *Trends Cell Biol.*, 2004, **14**, 497-504.
186. S. K. Bhunia, A. Saha, A. R. Maity, S. C. Ray and N. R. Jana, *Sci. Rep-UK*, 2013, **3**, DOI: 10.1038/srep01473.
187. B. S. Chen, F. M. Li, S. X. Li, W. Weng, H. X. Guo, T. Guo, X. Y. Zhang, Y. B. Chen, T. T. Huang, X. L. Hong, S. Y. You, Y. M. Lin, K. H. Zeng and S. Chen, *Nanoscale*, 2013, **5**, 1967-1971.
188. X. H. Zhu, H. Y. Wang, Q. F. Jiao, X. Xiao, X. X. Zuo, Y. Liang, J. M. Nan, J. F. Wang and L. S. Wang, *Part. Part. Syst. Char.*, 2014, **31**, 771-777.
189. G. S. Tong, J. X. Wang, R. B. Wang, X. Q. Guo, L. He, F. Qiu, G. Wang, B. S. Zhu, X. Y. Zhu and T. Liu, *J. Mater. Chem. B*, 2015, **3**, 700-706.
190. L. He, T. T. Wang, J. P. An, X. M. Li, L. Y. Zhang, L. Li, G. Z. Li, X. T. Wu, Z. M. Su and C. G. Wang, *Crystrngcomm*, 2014, **16**, 3259-3263.
191. S. Pandey, M. Thakur, A. Mewada, D. Anjarlekar, N. Mishra and M. Sharon, *J. Mater. Chem. B*, 2013, **1**, 4972-4982.
192. L. M. Hu, Y. Sun, S. L. Li, X. L. Wang, K. L. Hu, L. R. Wang, X. J. Liang and Y. Wu, *Carbon*, 2014, **67**, 508-513.
193. L. Cheng, Y. M. Li, X. Y. Zhai, B. Xu, Z. Q. Cao and W. G. Liu, *Acs Appl. Mater. Interfaces*, 2014, **6**, 20487-20497.
194. N. Gogoi and D. Chowdhury, *J. Mater. Chem. B*, 2014, **2**, 4089-4099.
195. J. Kim, J. Park, H. Kim, K. Singha and W. J. Kim, *Biomaterials*, 2013, **34**, 7168-7180.
196. S. Pandey, A. Mewada, M. Thakur, A. Tank and M. Sharon, *Rsc Adv.*, 2013, **3**, 26290-26296.
197. J. Wang, Z. H. Zhang, S. Zha, Y. Y. Zhu, P. Y. Wu, B. Ehrenberg and J. Y. Chen, *Biomaterials*, 2014, **35**, 9372-9381.
198. M. Zheng, S. Liu, J. Li, D. Qu, H. F. Zhao, X. G. Guan, X. L. Hu, Z. G. Xie, X. B. Jing and Z. C. Sun, *Adv. Mater.*, 2014, **26**, 3554-3560.

199. H. Wang, J. Shen, Y. Y. Li, Z. Y. Wei, G. X. Cao, Z. Gai, K. L. Hong, P. Banerjee and S. Q. Zhou, *Biomater. Sci.*, 2014, **2**, 915-923.
200. A. Chandra, S. Deshpande, D. B. Shinde, V. K. Pillai and N. Singh, *Acs Macro Lett.*, 2014, **3**, 1064-1068.
201. M. Nurunnabi, Z. Khatun, M. Nafiujjaman, D. G. Lee and Y. K. Lee, *Acs Appl. Mater. Interfaces*, 2013, **5**, 8246-8253.
202. Abdullah-Al-Nahain, J. E. Lee, I. In, H. Lee, K. D. Lee, J. H. Jeong and S. Y. Park, *Mol. Pharm.*, 2013, **10**, 3736-3744.
203. P. Nigam, S. Waghmode, M. Louis, S. Wangnoo, P. Chavan and D. Sarkar, *J. Mater. Chem. B*, 2014, **2**, 3190-3195.
204. Q. Liu, B. D. Guo, Z. Y. Rao, B. H. Zhang and J. R. Gong, *Nano Lett.*, 2013, **13**, 2436-2441.
205. X. T. Zheng, H. L. He and C. M. Li, *Rsc Adv.*, 2013, **3**, 24853-24857.
206. Z. H. Wang, J. F. Xia, C. F. Zhou, B. Via, Y. Z. Xia, F. F. Zhang, Y. H. Li, L. H. Xia and J. Tang, *Colloids Surf. B*, 2013, **112**, 192-196.
207. S. M. Chowdhury, C. Surhland, Z. Sanchez, P. Chaudhary, M. A. S. Kumar, S. Lee, L. A. Pena, M. Waring, B. Sitharaman and M. Naidu, *Nanomed-Nano.Technol.*, 2015, **11**, 109-118.
208. T. Chen, H. Yu, N. E. Yang, M. D. Wang, C. D. Ding and J. J. Fu, *J. Mater. Chem. B*, 2014, **2**, 4979-4982.
209. Y. J. Jing, Y. H. Zhu, X. L. Yang, J. H. Shen and C. Z. Li, *Langmuir*, 2011, **27**, 1175-1180.
210. B. Zheng, C. Wang, X. Z. Xin, F. Liu, X. J. Zhou, J. Y. Zhang and S. W. Guo, *J. Phys. Chem. C*, 2014, **118**, 7637-7642.
211. B. Z. Ristic, M. M. Milenkovic, I. R. Dakic, B. M. Todorovic-Markovic, M. S. Milosavljevic, M. D. Budimir, V. G. Paunovic, M. D. Dramicanin, Z. M. Markovic and V. S. Trajkovic, *Biomaterials*, 2014, **35**, 4428-4435.
212. H. J. Sun, N. Gao, K. Dong, J. S. Ren and X. G. Qu, *Acs Nano*, 2014, **8**, 6202-6210.
213. W. Y. Liu, J. C. Wei, Y. W. Chen, P. Huo and Y. Wei, *Acs Appl. Mater. Interfaces*, 2013, **5**, 680-685.
214. J. Li, Y. J. He, Z. He, P. Zeng and S. K. Xu, *Anal. Biochem.*, 2012, **428**, 4-6.
215. S. K. Sonkar, M. Ghosh, M. Roy, A. Begum and S. Sarkar, *Mater.Express*, 2012, **2**, 105-114.